Biochimica et Biophysica Acta 1828 (2013) 2083–2090

Contents lists available at SciVerse ScienceDirect

Biochimica et Biophysica Acta

journal homepage: www.elsevier.com/locate/bbamem

A bacterial monorhamnolipid alters the biophysical properties of phosphatidylethanolamine model membranes

Habib Abbasi [a], Francisco J. Aranda [c], Kambiz Akbari Noghabi [b], Antonio Ortiz [c,*]

[a] Department of Chemical Engineering, Jundi-Shapur University of Technology, Dezful, Iran
[b] Department of Molecular Genetics, National Institute of Genetic Engineering and Biotechnology (NIGEB), Tehran, Iran
[c] Department of Biochemistry and Molecular Biology-A, Veterinary Faculty, University of Murcia, E-30100 Murcia, Spain

ARTICLE INFO

Article history:
Received 4 October 2012
Received in revised form 16 April 2013
Accepted 17 April 2013
Available online 1 May 2013

Keywords:
Rhamnolipid
Dielaidoylphosphatidylethanolamine
Phospholipid vesicle
Differential scanning calorimetry
FTIR
SAXD

ABSTRACT

This work presents a biophysical study on the interactions of a monorhamnolipid (monoRL) produced by *Pseudomonas aeruginosa* MA01 with model dielaidoylphosphatidylethanolamine (DEPE) membranes. Incorporation of monoRL into DEPE shifts the onset temperature of the L_{β}-to-L_{α} and the L_{α}-to-H_{II} phase transitions toward lower values. Incorporation of monoRL into DEPE indicates the coexistence of lamellar and hexagonal–H_{II} phases in rhamnolipid-containing samples at 60 °C, at which pure DEPE is lamellar. Thus, both techniques show that monoRL facilitates formation of the hexagonal–H_{II} phase in DEPE, i.e. it destabilizes the bilayer organization. The phase diagram for the phospholipid component indicates a near-ideal behavior, with better miscibility of monoRL into DEPE in the fluid phase than in the gel phase. The various vibrational mode bands of the acyl chains of DEPE were studied by FTIR spectroscopy, focusing on the CH_2 symmetric stretching mode. Incorporation of monoRL into DEPE shifts the frequency of this band to higher wavenumbers, at temperatures both below and above the main gel to liquid–crystalline phase transition. Examination of the C═O stretching band of DEPE indicates that monoRL/DEPE interactions result in an overall dehydration effect on the polar headgroup of DEPE. These results are discussed in light of the possible role of rhamnolipids as bilayer stabilizers/destabilizers during cell membrane fluctuation events.

1. Introduction

Microorganisms are well known for the production of an increasing number of structurally diverse molecules of amphiphilic character [1–3], with very interesting potential applications [4]. Most of these compounds are known as biosurfactants, i.e., surface active molecules of biological origin. Currently, much effort is being dedicated to the search of new biosurfactants and to the application of biosurfactants in pharmaceutical formulations and in biomedicine [5,6], as antimicrobial agents [6,7], as additives in food and cosmetics [8,9], or in remediation technologies [10]. Within this context, it is clear that the characterization of the physicochemical and biological properties of biosurfactants is an essential step for the appropriate validation of these compounds in the abovementioned applications.

Pseudomonas aeruginosa, a Gram-negative bacterium well known for its environmental versatility, is able to cause disease in particular susceptible individuals. *P. aeruginosa* can utilize a wide range of organic compounds as substrates, thus conferring the microorganism an exceptional ability to colonize ecological niches, where nutrients are limited. Rhamnolipids constitute the main group of biosurfactants produced by *P. aeruginosa* when grown under appropriate conditions [11]. These glycolipid biosurfactants are composed of a hydrophilic head group constituted by one or two rhamnose molecules, called respectively monorhamnolipid (monoRL) (Fig. 1) and dirhamnolipid, and a hydrophobic tail formed by one or two fatty acids. The production of rhamnolipids shows high yields as compared to other biosurfactants [12], and used oils or wastes from the food industry can be used as carbon sources [8,13,14], the whole process being considered as a green process.

Studies on the interaction of the dirhamnolipid component, purified from the *P. aeruginosa* crude biosurfactant, with model phosphatidylcholine [15–18], and phosphatidylethanolamine membranes [19] have been recently carried out. Concerning the monoRL component, we have recently published on the physicochemical characteristics of the monomer-to-micelle transition of the *P. aeruginosa* monoRL [20], and its effect on model phosphatidylcholine membranes [21]. The abundance of phosphatidylethanolamine in biological membranes, and its capacity to promote non-bilayer structures have made this phospholipid a focus of attention for many years [22]. Dielaidoylphosphatidylethanolamine (DEPE), a major phospholipid found in an *Escherichia coli* fatty acid auxotroph, has been widely used as a model for unsaturated phosphatidylethanolamine species. The importance of nonbilayer lipids for protein function and the special packing properties of bilayers containing these lipids have been recently remarked [23]. This paper extends previous studies analyzing the molecular details on the interaction of monoRL

* Corresponding author. Tel.: +34 868 884788; fax: +34 868 884147.
E-mail address: ortizbq@um.es (A. Ortiz).

0005-2736/$ – see front matter © 2013 Elsevier B.V. All rights reserved.
http://dx.doi.org/10.1016/j.bbamem.2013.04.024

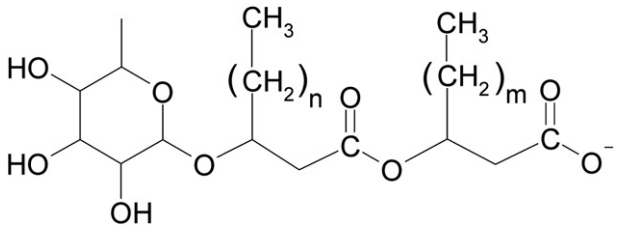

Fig. 1. The chemical structure of the monoRL compounds produced by *Pseudomonas aeruginosa* MA01. The predominant combinations of fatty acids found were: C_{10}–C_{10} (m, n = 6), C_{10}–C_{12} (m = 8, n = 6), and C_{10}–$C_{12:1}$ (m = 8, n = 6, one double bond).

with DEPE, establishing the relevant differences between dirhamnolipid and monoRL, and discussing the possible role of rhamnolipids in membrane stabilization/destabilization, and regulation of lipid polymorphism.

2. Materials and methods

2.1. Materials

Glucose, glycerol, sodium nitrate, potassium dihydrogen phosphate, magnesium sulfate, yeast extract, nutrient agar, ethyl acetate, hydrochloric acid, chromic acid, acetone, silica gel 60, chloroform, methanol and anthrone were purchased from Merck (Germany). Soybean oil was purchased from a local supermarket. Crude oil was obtained from the National Iranian Oil Company (NIOC). 1,2-Dielaidoyl-*sn*-glycero-3-phosphoethanolamine (DEPE) was from Avanti Polar Lipids Inc. (Birmingham, AL). All other reagents were of the highest purity available. Purified water was deionized using a Milli-Q equipment from Millipore (Millipore, Bedford, MA, USA) and had a resistivity of ca. 18 MΩ cm. Stock solutions of the phospholipid and the monoRL were prepared in chloroform/methanol (1:1) and stored at −20 °C. The buffers used through the work were aqueous 150 mM NaCl, 5 mM HEPES pH 7.4, and 150 mM NaCl, 5 mM HEPES pD 7.4 prepared in D_2O for the FTIR measurements. Water and all buffer solutions used in this work were filtered through 0.2 μm filters prior to use. The biosurfactant was produced, isolated and characterized as recently published [24].

2.2. Differential scanning calorimetry

Samples for DSC were prepared by dispersion of the required amounts of the phospholipid and the biosurfactant in the abovementioned aqueous buffer. Briefly, 3 μmol of DEPE and the corresponding amounts of monoRL, from stock solutions in chloroform/methanol (1:1), were mixed, and the solvent was gently evaporated under a stream of dry N_2, to obtain a thin film at the bottom of a glass tube. Last traces of the solvent were removed by a further minimum 3 h desiccation under vacuum. The abovementioned buffer (2 ml) was added to the dry samples and these were vortexed until a homogeneous suspension of multilamellar vesicles was obtained, always keeping the temperature above the gel to liquid–crystalline phase transition temperature of DEPE. Phospholipid phosphorus was determined by the method of Böttcher et al. [25]. Experiments were performed using a MicroCal MC2 calorimeter (MicroCal, Northampton, USA). The heating scan rate was 60 °C h^{-1}. The calorimeter was calibrated using pure phospholipids as standards.

Partial phase diagrams for the phospholipid component were constructed from the heating thermograms. The *solidus* and *fluidus* lines of the diagrams were defined by the onset and completion temperatures of the transition peaks obtained from heating scans. In order to avoid artifacts due to the thermal history of the sample the first scan was never considered. Second and further scans were carried out until a reproducible and reversible pattern was obtained, which usually occurred already with the second scan. The pretransitions were omitted from the diagrams for the sake of simplicity.

2.3. Fourier-Transform infrared spectroscopy

Samples for the Fourier-transform infrared (FTIR) spectroscopy measurements were prepared by mixing 10 μmol of DEPE and the corresponding amount of monoRL, from stock solutions in chloroform/methanol (1:1). The solvent was gently evaporated under a stream of dry N_2, to obtain a thin film at the bottom of a small glass tube, and last traces of the solvent were removed by a further minimum 3 h desiccation under vacuum. 100 μl of a 150 mM NaCl, 5 mM HEPES pD 7.4 buffer (in D_2O) was added to the dry samples and these were vortexed until a homogeneous suspension of multilamellar vesicles was obtained, always keeping the temperature above the gel to liquid–crystalline phase transition temperature of DEPE. An aliquot of the sample (approximately 20 μl), prepared as described above, was placed between two CaF_2 windows using 25 μm Teflon spacers, and the set was mounted in a thermostated cell holder. Infrared spectra were acquired in a Nicolet 6700 Fourier-transform infrared spectrometer (FTIR) (Madison, WI). Each spectrum was obtained by collecting 256 interferograms with a nominal resolution of 2 cm^{-1}. The equipment was continuously purged with dry air in order to minimize the contribution peaks of atmospheric water vapor. The sample holder was thermostated using a Peltier device (Proteus system from Nicolet). Spectra were collected at 2 °C intervals, allowing 5 min equilibration between temperatures. The D_2O buffer spectra taken at the same temperatures were subtracted interactively using either Omnic or Grams (Galactic Industries, Salem, NH) software. For examination of the C═O stretching band at various temperatures, the spectrum was zapped between 1780 and 1660 cm^{-1}, and the solvent baseline was subtracted. This C═O stretching band was fitted to its component bands by an iterative process using a Gaussian–Lorentzian function. The maxima of the component bands were set at 1742, 1728 and 1714 cm^{-1}, allowing a displacement of ±1 cm^{-1} during fitting.

2.4. Small-angle X-ray diffraction

Samples for X-ray diffraction analysis were prepared essentially as described above for DSC. Briefly, 10 μmol of DEPE and the corresponding amount of monoRL, from stock solutions in chloroform/methanol (1:1), were mixed. The solvent was gently evaporated under a stream of dry N_2, to obtain a thin film at the bottom of a small glass tube, and last traces of the solvent were removed by a further minimum 3 h desiccation under vacuum. 1 ml of a 150 mM NaCl, 5 mM HEPES pH 7.4 aqueous buffer was added to the dry samples and these were vortexed until a homogeneous suspension of multilamellar vesicles was obtained. The liposome suspensions were centrifuged in a bench microfuge and the pellets were placed in a steel holder, which provided good thermal contact to the Peltier heating unit, with cellophane windows. Typical exposure times were 5 min, allowing 10 min prior to the measurement for temperature equilibration. Small angle X-ray diffraction (SAXD) measurements were carried out using a Kratky compact camera (MBraum-Graz-Optical Systems, Graz, Austria) and a linear position sensitive detector (PSD; MBraum, Garching, Germany) monitoring the *s*-range ($s = 2 \sin\theta / \lambda$, 2θ = scattering angle, $\lambda = 1.54$ Å) between 0.0075 and 0.07 $Å^{-1}$. Nickel-filtered Cu K_α X-rays were generated by a Philips (Eindhoven, The Netherlands) PW3830 X-ray generator operating at 50 kV and 30 mA. The calibration of the detector position was performed by using silver stearate (d-spacing at 48.8 Å) as a reference material.

3. Results and discussion

There is no clear picture so far on which is the biological role played by the rhamnolipids secreted by *P. aeruginosa* and other bacteria. For some time it was accepted that these glycolipids played a role in the uptake of hydrophobic substrates by the bacterial cells, but more recent evidence strongly suggests that they primarily act as surface-associated stimuli [26]. In order to investigate which is the effect that rhamnolipids exert on the cell surface, the use of simpler model phospholipid vesicles could be of great help, given the complexity of the bacterial cell membrane. In this respect, we have recently reported on the interaction of the *P. aeruginosa* monoRL (Fig. 1) with various phosphatidylcholine membranes [21], and now this study is extended to model phosphatidylethanolamine membranes, the second most important phospholipid in biological membranes. DEPE was chosen to allow the simultaneous evaluation of the effect of monoRL on the lamellar gel to liquid–crystalline phase transition, as well as on the lamellar to hexagonal–H_{II} phase transition, a phase present in phosphatidylethanolamines but not in phosphatidylcholines under normal conditions.

3.1. Monorhamnolipid alters the thermotropic transitions of DEPE

Fig. 2 shows high sensitivity differential scanning calorimetry scans of DEPE in the absence and presence of increasing concentrations of monoRL. In the absence of monoRL, DEPE exhibited a highly cooperative and high enthalpy lamellar gel to liquid–crystalline (L_β-to-L_α) phase transition with a T_c at 37.0 °C, in agreement with previous data [19,27]. In addition DEPE also exhibited a low enthalpy lamellar liquid–crystalline to inverted hexagonal–H_{II} (L_α-to-H_{II}) phase transition with T_c of 60.8 °C, a value for the equilibrium phase transition which falls in the middle of the range 57.3–66 °C reported by several authors [19,27–31]. Both transitions were fully reversible on heating and cooling, as checked by successive scans of the same sample. Incorporation of increasing proportions of monoRL into DEPE shifted the onset temperature of the L_β-to-L_α phase transition to lower values, whereas the completion temperature was less affected. At concentrations above 0.05 mol fraction, this transition became very asymmetric, with a wide lower melting portion, and sharper higher temperature transition. The overall transition was still observable up to the highest concentration of monoRL assayed (0.2 mol fraction).

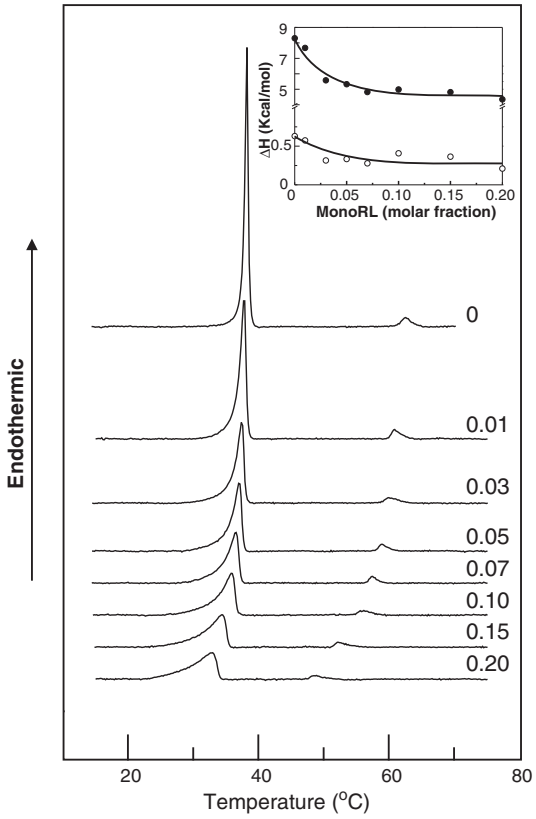

Fig. 2. DSC heating thermograms for DEPE in the presence of increasing concentrations of monoRL (number on the curves, molar fraction). Thermograms are normalized to the same amount of phospholipid. Inset: Enthalpy change for the gel to liquid–crystalline phase transition (closed circles) and the lamellar to hexagonal–H_{II} phase transition of DEPE (open circles) as a function of monoRL concentration.

The effect of monoRL on the L_α-to-H_{II} phase transition was similar, shifting the onset and completion temperatures toward lower values. At a 0.20 monoRL mol fraction this transition was still detectable by high sensitivity DSC.

Increasing the concentration of monoRL into DEPE resulted in a progressive decrease of the enthalpy change, ΔH, of both the gel to liquid–crystalline and the lamellar-to-hexagonal–H_{II} phase transitions (see Fig. 2 inset). The effect was not very intense, and ΔH did not further decrease at monoRL concentrations above a 0.10 mol fraction.

3.2. Monorhamnolipid modifies the phases adopted by DEPE

The effect of incorporation of monoRL on the phase adopted by DEPE dispersions and its characteristics was studied by performing SAXD (Fig. 3) and WAXD (Fig. 4) measurements. Phospholipids organized into multilamellar structures give rise to diffractograms with SAXD reflections which positions relate as 1:1/2:1/3:1/4:1 … [32], and the largest first-order reflection component corresponds to the interlamellar repeat distance, *d*, which is comprised of the bilayer thickness and the thickness of one adjacent interlamellar water layer [33]. The pattern for inverted hexagonal–H_{II} structures is 1: 1/√3: 1/√4: 1/√7 … [32], and the largest first-order reflection is related to the size of the hexagonal tubes. Nevertheless, in the case of lamellar DEPE only one sharp reflection was observed both below and above the gel to liquid–crystalline phase transition, i.e., no higher-order reflections were found, in agreement with previously reported data [34,35]. Thus, pure DEPE in the gel phase (25 °C) showed a first-order reflection with an interlamellar repeat distance of 64.6 Å, which decreased to 53.7 Å in the fluid state (45 °C) (Fig. 3), due to a decrease in the effective acyl chain length, or in the thickness of the hydration layer between bilayers. Only in the gel phase, at 25 °C, incorporation of monoRL into DEPE gave rise to the appearance of a second reflection at 59 Å which became more intense upon increasing the concentration. This might correspond to a second gel phase, enriched in monoRL, compatible with the highly asymmetric thermograms observed at these concentrations (see Fig. 2).

Pure DEPE showed a single reflection at all temperatures studied, except at 70 °C at which four reflections, which related as 1: 1/√3: 1/√4: 1/√7, were present, indicating a pure hexagonal–H_{II} phase. At 60 °C, pure DEPE showed a single reflection at 52.2 Å (lamellar liquid–crystalline). Upon addition of a 0.07 mol fraction of monoRL the characteristic reflections of the hexagonal–H_{II} phase were also present, indicating coexistence of both phases, i.e., monoRL was inducing the hexagonal–H_{II} phase at temperatures at which pure DEPE was lamellar.

Thus, with respect to the formation of the inverted hexagonal–H_{II} phase it was clear that monoRL shifted this transition toward lower temperatures, i.e. facilitated H_{II} phase formation or, in other words, destabilized the bilayer organization. According to the dynamic shape theory [36], these results showed that monoRL behaved as a cone shaped molecule which, by adding to the cone shape of DEPE, conferred positive curvature, and acted as a lamellar destabilizer. The opposite effect was described for the *P. aeruginosa* dirhamnolipid [19], for which a 0.10 mol fraction sample was still fully lamellar at

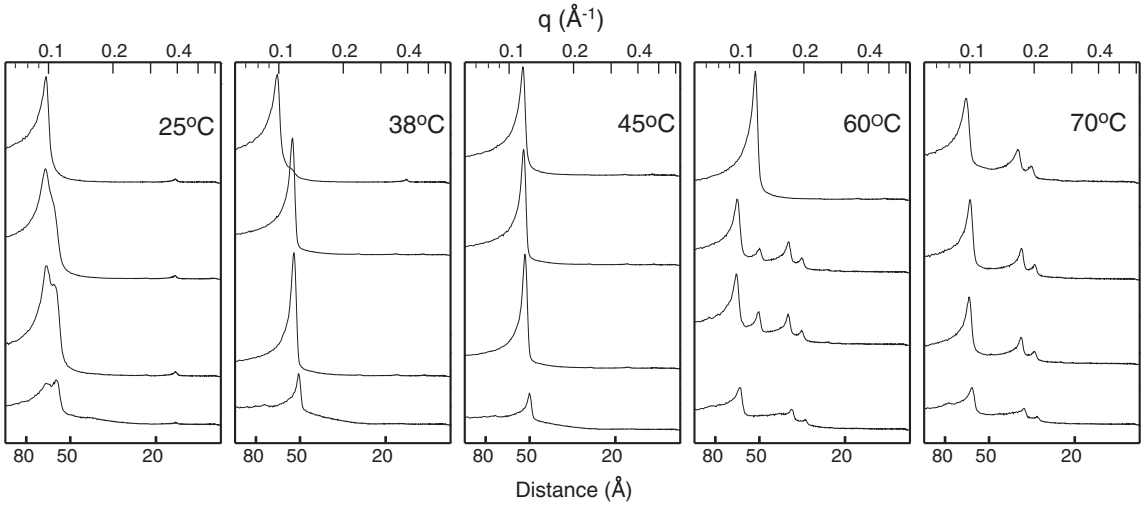

Fig. 3. Small angle X-ray diffraction profiles for pure DEPE, and in the presence of 0.01, 0.07 and 0.20 mol fraction of monoRL (from top to bottom). Measurements were carried out at the indicated temperatures.

70 °C. This difference is compatible with the pronounced inverted cone shape of dirhamnolipid, with a bulky polar disaccharide moiety, as compared to the single rhamnose of monoRL. These results are in good agreement with previous data showing that monoglucosyl [37] and monogalactosyl [38] diglycerides adopt hexagonal–H_{II} phases, whereas diglucosyl [37] and digalactosyl diglycerides [38] adopt lamellar phases, i.e. monosaccharide lipids facilitated H_{II}-phase formation, whereas disaccharide lipids inhibited H_{II}-phase formation.

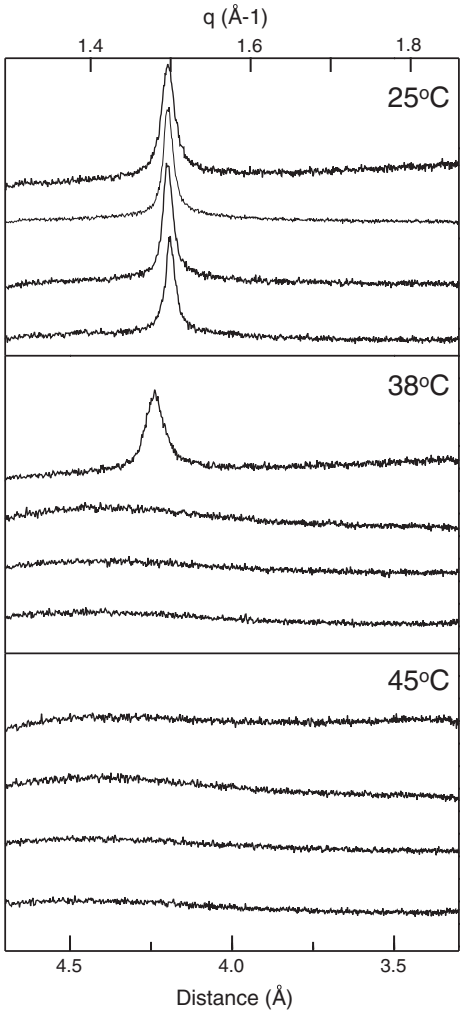

Fig. 4. Wide angle X-ray diffraction profiles of pure DEPE, and in the presence of 0.01, 0.07 and 0.20 mol fraction of monoRL (from top to bottom) at various temperatures.

Information about the packing of the DEPE acyl chains was obtained through WAXD measurements. Fig. 4 shows the WAXD pattern corresponding to pure DEPE and DEPE containing monoRL at various temperatures. At 25 °C pure DEPE showed a single sharp symmetric reflection centered at 4.20 Å indicating that the hydrocarbon chains were packed in a hexagonal lattice and the direction of the chains was normal to the membrane surface, characteristic of the untilted gel phase [39,40]. At 38 °C, whereas pure DEPE was still in the gel phase, monoRL-containing samples showed a very broad component centered at approx. 4.4 Å, instead of any sharp reflection, characteristic of the fluid liquid–crystalline phase [39,40]. At 45 °C all samples showed the typical fluid liquid–crystalline diffraction pattern.

3.3. Phase diagram of monoRL/DEPE system

Using the thermal data from the DSC scans shown in Fig. 2, and the phase assignment from SAXD (Fig. 3), a partial phase diagram for the phospholipid component was constructed (Fig. 5), including the L_β-to-L_α and the L_α-to-H_{II} phase transitions. Increasing the concentration of monoRL gave rise to a moderate decrease in the *fluidus* line which behaved in a near ideal manner. The *solidus* line also decreased, according to an essentially near ideal behavior. Both lines were more separated upon increasing monoRL concentration, indicating a loss of cooperativity of the transition. The diagram showed good miscibility of monoRL and DEPE in the solid and fluid phases, within the whole range of concentrations studied. In the case of the corresponding dirhamnolipid compound [19], there was a region of gel immiscibility in the phase diagram, showing that the pronounced inverted cone shape of the dirhamnolipid conferred it a tendency to segregate from DEPE in the gel phase.

The boundary lines of the L_α-to-H_{II} phase transition decreased their temperature upon increasing monoRL concentration. Both lines were essentially parallel in the whole range of concentration, indicating that the cooperativity of the transition was maintained upon increasing monoRL concentration. It was clearly shown in this diagram that increasing monoRL concentration shifted the L_α-to-H_{II} phase transition boundaries to lower temperatures, i.e., it stabilized the H_{II} phase.

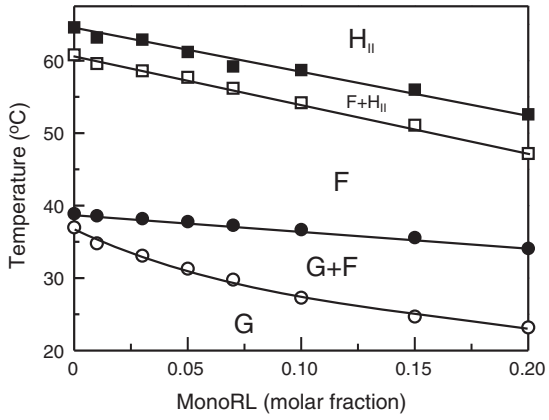

Fig. 5. Partial phase diagram for the phosphatidylethanolamine component of mixtures monoRL/DEPE. Closed (*solidus* line) and open (*fluidus* line) circles were obtained from the onset and completion temperatures of the main gel to liquid–crystalline phase transitions, and closed and open squares were obtained from the onset and completion temperatures of the lamellar to hexagonal–H_{II} phase transitions shown in Fig. 2. The phase designations are as follows: G (L_{β}, gel phase), F (L_{α}, liquid–crystalline phase), and H_{II} (inverted hexagonal–H_{II} phase).

3.4. Fourier-transform infrared spectroscopy

FTIR allowed investigation of the molecular interactions of monoRL with the various functional groups of the DEPE molecule, characteristics of the polar headgroup or the acyl chain regions. The L_{β}-to-L_{α} phase transition involves large structural changes, with the introduction of conformational disorder (*gauche* conformers), which are reflected in the infrared spectrum. Upon melting there is an effect on the frequency of the band that can be correlated with a higher population of *gauche* conformers of the phospholipid in the liquid–crystalline phase. The various vibrational mode bands of the acyl chains of DEPE were examined, although only the CH_2 symmetric stretching mode at ca. 2850 cm^{-1} will be shown, since no additional information could be gained from the other bands. The temperature dependence of the maximum of the symmetric CH_2 stretching band is shown in Fig. 6 for pure DEPE and DEPE containing monoRL. Pure DEPE showed two increases in wavenumber, the first one corresponding to the gel to liquid–crystalline acyl chain melting transition, and the second to the additional conformational disorder introduced by the lamellar to hexagonal–H_{II} transition, in accordance to previous work on non bilayer transitions in phosphatidylethanolamines [41]. Upon incorporation of increasing concentrations of monoRL there was a broadening and shift to lower temperatures of the transition, in agreement with the DSC results. The

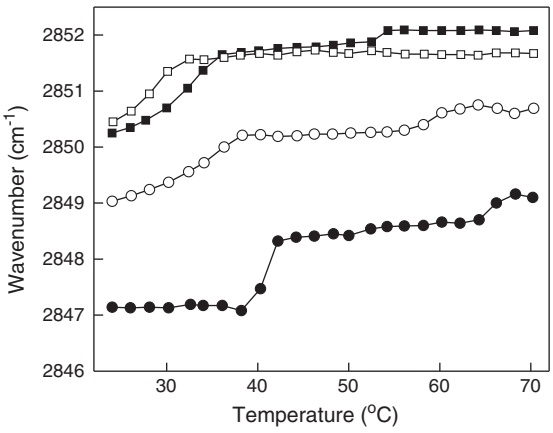

Fig. 6. Temperature dependence of the maximum of the CH_2 symmetric stretching absorption band for pure DEPE (●), and in the presence of 0.07 (○), 0.10 (■) and 0.20 (□) mol fraction of monoRL.

increase in the frequency of this band induced by monoRL, both below and above the phase transition temperature, is associated with an overall increase in the conformational disorder of the hydrocarbon chains of DEPE, and has been reported before for other glycolipid biosurfactants [42].

Vibrational modes of the functional groups found in the headgroup of phospholipids give rise to a number of infrared bands, from which the carbonyl stretching absorption is the most useful [38], particularly for the study of the hydration of phospholipid assemblies [43,44]. The C═O groups of diacylphospholipids in lipid vesicles may be in a hydrated and a dehydrated state, and the proportion of both fractions usually depends on the physical state of the phospholipid bilayer [45,46]. Thus, the spectrum of most phospholipids represents a summation of two component bands centered near 1742 and 1727 cm^{-1}, and attributed to dehydrated (non hydrogen-bonded) and hydrated (hydrogen-bonded) C═O groups, respectively [47]. However the contours of the C═O stretching bands of some phosphatidylethanolamines, like DEPE, are much wider and only resolvable into at least three component bands centered around 1742, 1728 and 1714 cm^{-1}. The additional band at 1714 cm^{-1} is indicative of another population of hydrogen-bonded C═O groups, which is not present in hydrated phosphatidylcholine bilayers [48]. Fig. 7 shows the C═O stretching band of DEPE in the absence and presence of monoRL, both below and above the gel to liquid–crystalline phase transition temperature. Pure DEPE at 28 °C showed a band centered around 1736 cm^{-1}, which shifted down to 1726 cm^{-1} upon melting, concomitantly with a widening of the band contour due to the higher hydration of the lipid/water interface in the liquid–crystalline state. Incorporation of 0.10 monoRL mol fraction shifted the maximum of this band to 1738.7 and 1735 cm^{-1} below and above the phase transition temperature, respectively. It was also observed that the C═O stretching band was widened toward the low frequency side. Both effects indicated that monoRL decreased the hydration of the polar headgroup of DEPE both in the L_{β} and the L_{α} phases. To quantify this effect, the C═O stretching bands were subjected to band fitting to obtain the component bands (Fig. 7, dashed lines). These bands could be accurately fitted to the three bands centered at 1742, 1728 and 1714 cm^{-1}, commented above. The results obtained are shown in Table 1. In the L_{β} phase, addition of monoRL increased the 1742 cm^{-1}, and decreased the 1729 and 1714 cm^{-1} component bands. The overall effect was a strong dehydration of the interface induced by monoRL. In the fluid L_{α} phase, incorporation of monoRL increased the 1742 cm^{-1} component, the 1729 cm^{-1} component remained essentially unaffected, and the 1714 cm^{-1} band was considerably decreased. The global effect was a shift of the maximum frequency toward higher wavenumbers, also indicating dehydration as compared to the pure phospholipid. In hydrated phosphatidylethanolamine bilayers, at difference with phosphatidylcholines, there are two possible hydrogen-bonding donors: interfacial water and the NH_2 protons of the phosphorylethanolamine headgroup. It has been argued that probably the 1729 cm^{-1} component arises from hydrogen bonding to interfacial water, whereas the 1714 cm^{-1} band corresponds to hydrogen bonding to the headgroup amine group [48]. Within this scenario, the effect of monoRL/DEPE interactions results in a reorganization of the hydrogen bonding pattern, with decreased water hydrogen-bonding and a concomitant decrease in amine group hydrogen-bonding. The three hydroxyl groups of monoRL will probably establish a large number of hydrogen interactions with water molecules, leaving less water available to interact with the phospholipid. The loss in water hydrogen-bonding could result in a reduction of the hydration layer width, contributing to explain the decrease in *d*-spacing observed in SAXD measurements described above.

Fig. 8 shows the temperature dependence of the maximum frequency of the C═O stretching band of DEPE pure and in the presence of monoRL. In agreement with previous report on the infrared characterization of phase transitions of phosphatidylethanolamines [41], the maximum of the C═O stretching band of pure DEPE decreased during the gel to liquid–crystalline phase transition, which was consistent

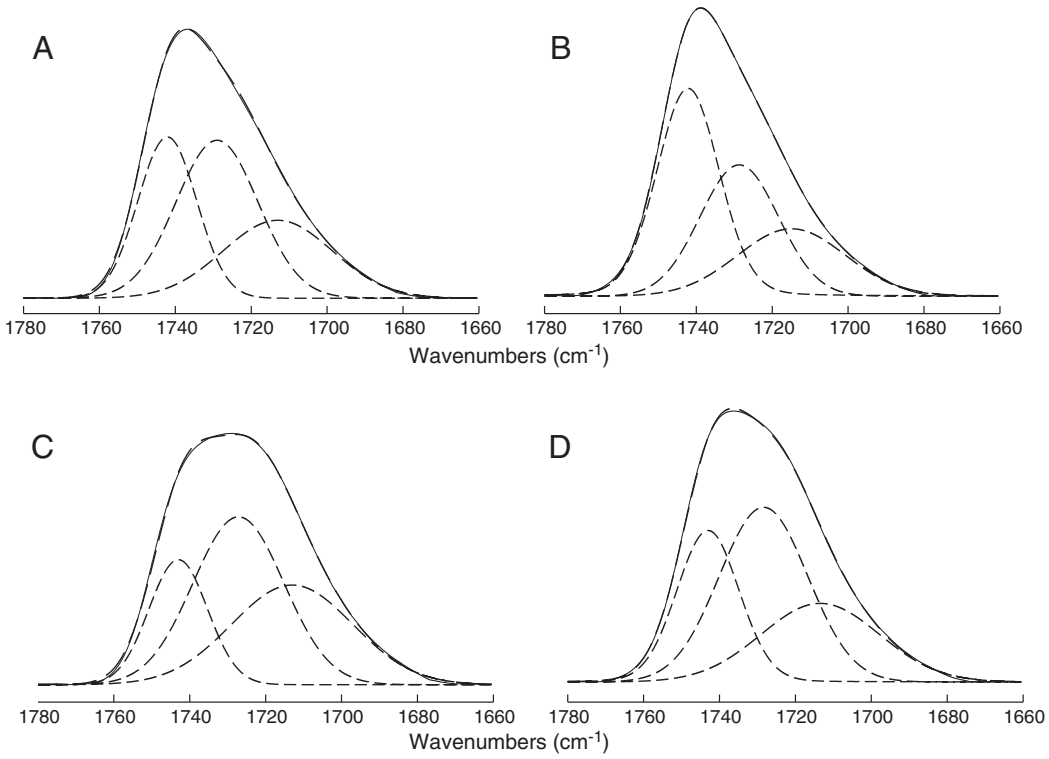

Fig. 7. The C═O stretching region of the FTIR spectra of DEPE. Spectra correspond to DEPE at 28 °C in the absence (A) and presence of a 0.10 mol fraction of monoRL (B), and DEPE at 50 °C in the absence (C) and presence of a 0.10 mol fraction of monoRL (D). Solid lines are the original spectra, long-dashed lines are the fitted spectra, and short-dashed lines correspond to the component bands obtained by band fitting.

with the increase in the lower frequency component of the C═O band resulting in an increase in hydration (Table 1). On the other hand, the lamellar to hexagonal–H_{II} phase transition was accompanied by an increase of the frequency maximum, which indicated the dehydration taking place during the formation of the inverted phase [49]. It can be observed that incorporation of monoRL shifted the temperature of both transitions to lower values, in agreement with DSC results, and only in the 0.20 monoRL mol fraction sample there was no shift in the H_{II} transition. Taking together, the described effects on the modulation of the DEPE/water interface by monoRL in the biologically most significant L_α phase, indicate that monoRL interaction leads to conformational changes in DEPE resulting in decreasing water hydrogen-bonding and amine group hydrogen-bonding.

4. Conclusions

The data presented and discussed above have shown that a bacterial monoRL interacts with DEPE model membranes, destabilizes the lamellar configuration, and perturbs the characteristics of the lipid/water interface, by modification of the hydrogen-bonding pattern.

Table 1
The proportion of the components of the C═O stretching band of DEPE in the absence and presence of monoRL. Data corresponding to one representative experiment are shown.

Sample	Temperature	Component band (%)		
		1742 cm^{-1}	1729 cm^{-1}	1714 cm^{-1}
DEPE	28 °C	30.5	42.0	27.5
DEPE + 0.10 monoRL mol fraction		43.2	33.2	23.5
DEPE	50 °C	20.8	44.4	34.7
DEPE + 0.10 monoRL mol fraction		28.0	45.0	27.0

The question as to the biological role of the rhamnolipids secreted by *P. aeruginosa* remains unclear. The old agreement on its role facilitating bacteria growing on hydrophobic substrates [50], or as a defensive mechanism [51], has been progressively substituted by the idea that they might act as surface-associated stimuli [26]. Thus, it has been shown that rhamnolipids are involved in the swarming motility behavior [52], and structural biofilm development [53] in *P. aeruginosa*. The amphiphilic nature of rhamnolipids results in a propensity to accumulate at interfaces, and then probably act as surface-specific stimuli [52]. The effect of monoRL on the interfacial region of phosphatidylethanolamine bilayers, as well as on DEPE lipid polymorphism, might well help to explain the molecular basis of the roles commented above. In addition, in light of our results,

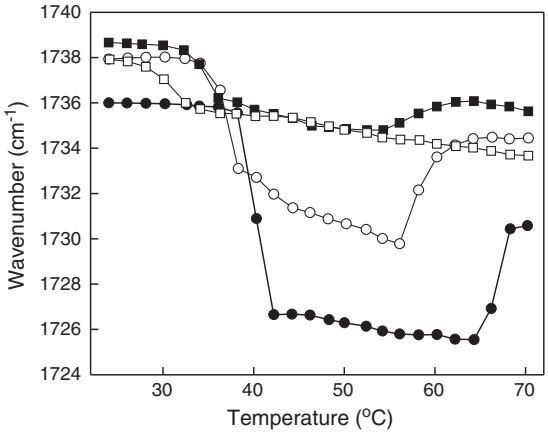

Fig. 8. Temperature dependence of the maximum of the C═O stretching absorption band for pure DEPE (●), and in the presence of 0.07 (○), 0.10 (■) and 0.20 (□) mol fraction of monoRL.

another biological role could be tentatively attributed to rhamnolipids. The existence of phosphatidylethanolamine lipid domains in bacterial cell membranes, with the propensity of phosphatidylethanolamine to form non-bilayer structures, suggests that these domains may play a role in controlling morphological changes during cell division [54,55]. In fact, fusion and fission of bilayer membranes might require a lipid to take on a non-bilayer structure [36], and a big challenge for the cell during these fusion and fission events is to maintain its integrity. Our results on the interaction of monoRL with DEPE show a strong destabilization of lamellar structures by the glycolipid, as compared to the stabilizing effect of the dirhamnolipid component [19]. Since the maximum rates of rhamnolipid production occur during the growth phase [56], where maximum cell division is taking place, and rhamnolipids are sequentially synthesized, first monoRL and second dirhamnolipid, it is possible that the transient time-dependent association between the various rhamnolipids and cell membranes might help to coordinate the cell membrane fluctuations events taking place during cell division events.

Acknowledgements

We want to thank Prof. J.A. Teruel for helpful discussions. This work was supported by project No. CTQ2007-66244 (to A.O.) from the Spanish Ministry of Science and Innovation (MCINN).

References

[1] J.D. Desai, I.M. Banat, Microbial production of surfactants and their commercial potential, Microbiol. Mol. Biol. Rev. 61 (1997) 47–64.
[2] P. Singh, S.S. Cameotra, Potential applications of microbial surfactants in biomedical sciences, Trends Biotechnol. 22 (2004) 142–146.
[3] L. Rodrigues, I.M. Banat, J.A. Teixeira, R. Oliveira, Biosurfactants: potential applications in medicine, J. Antimicrob. Chemother. 57 (2006) 609–618.
[4] A.K. Mukerjee, K. Das, Microbial surfactants and their potential applications, Adv. Exp. Med. Biol. 672 (2010) 54–64.
[5] T. Stipcevic, T. Piljac, R.R. Isseroff, Di-rhamnolipid from *Pseudomonas aeruginosa* displays differential effects on human keratinocyte and fibroblast cultures, J. Dermatol. Sci. 40 (2005) 141–143.
[6] L. Rodrigues, J.A. Teixeira, Microbial biosurfactants and biodegradation, Adv. Exp. Med. Biol. 672 (2010) 65–74.
[7] M. Benincasa, A. Abalos, I. Oliveira, A. Manresa, Chemical structure, surface properties and biological activities of the biosurfactant produced by *Pseudomonas aeruginosa* LBI from soapstock, Antonie Van Leeuwenhoek 85 (2004) 1–8.
[8] S. Lang, D. Wullbrandt, Rhamnose lipids—biosynthesis, microbial production and applications potential, Appl. Microbiol. Biotechnol. 51 (1999) 22–32.
[9] R.M. Maier, G. Soberón-Chavez, *Pseudomonas aeruginosa* rhamnolipids: biosynthesis and potential applications, Appl. Microbiol. Biotechnol. 54 (2000) 625–633.
[10] A. Franzetti, E. Tamburini, I.M. Banat, Application of biological surface active compounds in remediation technologies, Adv. Exp. Med. Biol. 672 (2010) 121–134.
[11] F.G. Jarvis, M.J. Johnson, A glycolipid produced by *Pseudomonas aeruginosa*, J. Am. Chem. Soc. 71 (1949) 4124–4126.
[12] M. Benincasa, A.M. Marqués, A. Pinazo, A. Manresa, Rhamnolipid surfactants: alternative substrates, new strategies, Adv. Exp. Med. Biol. 672 (2010) 170–184.
[13] I.M. Banat, R.S. Makkar, S.S. Cameotra, Potential applications of microbial surfactants, Appl. Microbiol. Biotechnol. 53 (2000) 495–508.
[14] G. Soberón-Chávez, F. Lépine, E. Déziel, Production of rhamnolipids by *Pseudomonas aeruginosa*, Appl. Microbiol. Biotechnol. 14 (2005) 1–8.
[15] A. Ortiz, J.A. Teruel, M.J. Espuny, A. Marqués, A. Manresa, F.J. Aranda, Effects of dirhamnolipid on the structural properties of phosphatidylcholine membranes, Int. J. Pharm. 325 (2006) 99–107.
[16] F.J. Aranda, M.J. Espuny, A. Marqués, J.A. Teruel, A. Manresa, A. Ortiz, Thermodynamics of the interaction of a dirhamnolipid biosurfactant secreted by *Pseudomonas aeruginosa* with phospholipid membranes, Langmuir 23 (2007) 2700–2705.
[17] M. Sánchez, F.J. Aranda, J.A. Teruel, A. Ortiz, Interaction of a bacterial dirhamnolipid with phosphatidylcholine membranes: a biophysical study, Chem. Phys. Lipids 161 (2009) 51–55.
[18] A. Ortiz, F.J. Aranda, J.A. Teruel, Interaction of dirhamnolipid biosurfactants with phospholipid membranes: a molecular level study, Adv. Exp. Med. Biol. 672 (2010) 42–53.
[19] M. Sánchez, J.A. Teruel, M.J. Espuny, A. Marqués, F.J. Aranda, A. Manresa, A. Ortiz, Modulation of the physical properties of dielaidoylphosphatidylethanolamine membranes by a dirhamnolipid biosurfactant produced by *Pseudomonas aeruginosa*, Chem. Phys. Lipids 142 (2006) 118–127.
[20] H. Abbasi, K.A. Noghabi, M.M. Hamedi, H.S. Zahiri, A.A. Moosavi-Movahedi, M. Amanlou, J.A. Teruel, A. Ortiz, Physicochemical characterization of a monorhamnolipid secreted by *Pseudomonas aeruginosa* MA01 in aqueous media. An experimental and molecular dynamics study, Colloids Surf. B 101 (2013) 256–265.
[21] H. Abbasi, K.A. Noghabi, A. Ortiz, Interaction of a bacterial monorhamnolipid secreted by *Pseudomonas aeruginosa* MA01 with phosphatidylcholine model membranes, Chem. Phys. Lipids 165 (2012) 745–752.
[22] J.E. Vance, Phosphatidylserine and phosphatidylethanolamine in mammalian cells: two metabolically related aminophospholipids, J. Lipid Res. 49 (2008) 1377–1387.
[23] R.M. Epand, Membrane lipid polymorphism: relationship to bilayer properties and protein function, Methods Mol. Biol. 400 (2007) 15–26.
[24] H. Abbasi, M.M. Hamedi, T.B. Lotfabad, H.S. Zahiri, H. Sharafi, F. Masoomi, A.A. Moosavi-Movahedi, A. Ortiz, M. Amanlou, K.A. Noghabi, Biosurfactant-producing bacterium, *Pseudomonas aeruginosa* MA01 isolated from spoiled apples: physicochemical and structural characteristics of isolated biosurfactant, J. Biosci. Bioeng. 113 (2012) 211–219.
[25] C.J.F. Böttcher, C.M. Van Gent, C. Pries, A rapid and sensitive sub-micro phosphorus determination, Anal. Chim. Acta 24 (1961) 203–204.
[26] L. Chrzanoswki, L. Lawniczak, K. Czaczyk, Why do microorganisms produce rhamnolipids? World J. Microbiol. Biotechnol. 28 (2012) 401–419.
[27] T.P.W. McMullen, R.N. McElhaney, Differential scanning calorimetric studies of the interaction of cholesterol with distearoyl and dielaidoyl molecular species of phosphatidylcholine, phosphatidylethanolamine, and phosphatidylserine, Biochemistry 36 (1997) 4979–4986.
[28] N.M. Tsvetkova, I. Horvath, Z. Torok, W.F. Wolkers, Z. Balogi, N. Shigapova, L.M. Crowe, F. Tablin, E. Viertling, J.H. Crowe, L. Vigh, Small heat-shock proteins regulate membrane lipid polymorphism, Proc. Natl. Acad. Sci. U. S. A. 99 (2002) 13504–13509.
[29] F. Liu, R.N.A.H. Lewis, R.S. Hodges, R.N. McElhaney, A differential scanning calorimetric and ^{31}P NMR spectroscopic study of the effect of transmembrane α-helical peptides on the lamellar-reversed hexagonal phase transition of phosphatidylethanolamine model membranes, Biochemistry 40 (2001) 760–768.
[30] R. Koynova, B. Tenchov, G. Rapp, Low amounts of PEG-lipid induce cubic phase in phosphatidylethanolamine dispersions, Biochim. Biophys. Acta 1326 (1997) 167–170.
[31] P.L. Cook, J.L. Vanderhill, A.E. Cook, D.W. Van Norstrand, M.T. Gordon, P.E. Harper, Light scattering measurement and Avrami analysis of the lamellar to inverse hexagonal phase transition kinetics of the lipid DEPE, Chem. Phys. Lipids 165 (2012) 270–276.
[32] V. Luzzati, X-Ray diffraction studies of lipid–water systems, in: D. Chapman (Ed.), Biological Membranes, Academic Press, New York, 1968, pp. 71–123.
[33] M. Rappolt, A. Hickel, F. Brigenzu, K. Lohner, Mechanism of the lamellar/inverse hexagonal phase transition examined by high resolution X-ray diffraction, Biophys. J. 84 (2003) 3111–3122.
[34] J.A. Killian, B. De Kruijff, Thermodynamic, motional and structural aspects of gramicidin-induced hexagonal H_{II} phase formation in phosphatidylethanolamine, Biochemistry 24 (1985) 7881–7890.
[35] A. Ortiz, F.J. Aranda, The influence of vitamin K_1 on the structure and phase behaviour of model membrane systems, Biochim. Biophys. Acta 1418 (1999) 206–220.
[36] P.R. Cullis, B. De Kruijff, Lipid polymorphism and the functional roles of lipids in biological membranes, Biochim. Biophys. Acta 559 (1979) 399–420.
[37] A. Wieslander, J. Ulmius, G. Lindblom, K. Fontell, Water binding and phase structure for different *Acholeplasma laidlawii* membrane lipids studied by deuteron magnetic resonance and X-ray diffraction, Biochim. Biophys. Acta 512 (1978) 241–253.
[38] G.G. Shipley, J.P. Green, B.W. Nichols, The phase behavior of monogalactosyl, digalactosyl and sulphoquinovosyl diglycerides, Biochim. Biophys. Acta 311 (1973) 531–544.
[39] J.M. Seddon, K. Harlos, D. Marsh, Metastability and polymorphism in the gel and fluid bilayer phases of dilauroylphosphatidylethanolamine. Two crystalline forms in excess water, J. Biol. Chem. 25 (1983) 3850–3854.
[40] A. Tardieu, V. Luzzati, F.C. Reman, Structure and polymorphism of the hydrocarbon chains of lipids: a study of lecithin–water phases, J. Mol. Biol. 25 (1973) 711–733.
[41] H.H. Manstch, A. Martin, D.G. Cameron, Characterization by infrared spectroscopy of the bilayer to nonbilayer phase transition of phosphatidylethanolamines, Biochemistry 20 (1981) 3138–3145.
[42] A. Ortiz, J.A. Teruel, M.J. Espuny, A. Marqués, A. Manresa, F.J. Aranda, Interactions of a *Rhodococcus* sp. biosurfactant trehalose lipid with phosphatidylethanolamine membranes, Biochim. Biophys. Acta 1778 (2008) 2806–2813.
[43] H.L. Casal, H.H. Mantsch, Polymorphic phase behavior of phospholipid membranes studied by infrared spectroscopy, Biochim. Biophys. Acta 779 (1984) 381–401.
[44] W. Pohle, C. Selle, H. Fritzsche, H. Binder, Fourier Transform infrared spectroscopy as a probe for the study of the hydration of lipid self-assemblies. I. Methodology and general phenomena, Biospectroscopy 4 (1998) 267–280.
[45] A. Blume, W. Hübner, G. Messner, Fourier transform infrared spectroscopy of ^{13}C═O-labeled phospholipids hydrogen bonding to carbonyl groups, Biochemistry 27 (1988) 8239–8249.
[46] R.N.A.H. Lewis, R.N. McElhaney, W. Pohle, H.H. Mantsch, Components of the carbonyl stretching band in the infrared spectra of hydrated 1,2-diacylglycerolipid bilayers: a reevaluation, Biophys. J. 67 (1994) 2367–2375.
[47] H.H. Mantsch, R.N. McElhaney, Phospholipid phase transitions in model and biological membranes as studied by infrared spectroscopy, Chem. Phys. Lipids 57 (1991) 213–226.
[48] R.N.A.H. Lewis, R.N. McElhaney, Calorimetric and spectroscopic studies of the polymorphic phase behavior of a homologous series of n-saturated 1,2-diacylphosphatidylethanolamines, Biophys. J. 64 (1993) 1081–1096.
[49] J. Katsaras, K.R. Jeffrey, D.S.-C. Yang, R.M. Epand, Direct evidence for the partial dehydration of phosphatidylethanolmine bilayers of approaching the hexagonal phase, Biochemistry 32 (1993) 10700–10707.
[50] A. Fiechter, Biosurfactants: moving towards industrial application, Trends Biotechnol. 10 (1992) 208–217.

[51] M.E. Stanghellini, R.M. Miller, Biosurfactants—their identity and potential efficacy in the biological control of zoosporic plant pathogens, Plant Dis. 81 (1997) 4–12.
[52] J. Tremblay, A.P. Richardson, F. Lépine, E. Déziel, Self-produced extracellular stimuli modulate the *Pseudomonas aeruginosa* swarming motility behavior, Environ. Microbiol. 9 (2007) 2622–2630.
[53] S.J. Pamp, T. Tolker-Nielsen, Multiple roles of biosurfactants in structural biofilm development by *Pseudomonas aeruginosa*, J. Bacteriol. 189 (2007) 2531–2539.
[54] K. Matsumoto, J. Kusaka, A. Nishibori, H. Hara, Lipid domains in bacterial membranes, Mol. Microbiol. 61 (2006) 1110–1117.
[55] R.M. Epand, R.F. Epand, Domains in bacterial membranes and the action of antimicrobial agents, Mol. Biosyst. 5 (2009) 580–587.
[56] M.M. Müller, R. Hausmann, Regulatory and metabolic network of rhamnolipid biosynthesis: traditional and advanced engineering towards biotechnological production, Appl. Microbiol. Biotechnol. 91 (2011) 251–264.